https://doi.org/10.46813/2023-144-024

MORPHOLOGICAL CHARACTERISTICS OF CRATERS ON THE SURFACE OF AA1933 ALUMINUM ALLOY IRRADIATED BY PULSED ELECTRON BEAM

V.V. Bryukhovetsky[1], V.V. Lytvynenko[1], Yu.F. Lonin[2], D.E. Myla[1,3], A.G. Ponomarev[2], V.T. Uvarov[2]
[1]Institute of Electrophysics and Radiation Technologies NAS of Ukraine, Kharkiv, Ukraine
E-mail: ntcefo@yahoo.com;
[2]NSC "Kharkov Institute of Physics and Technology" Kharkiv, Ukraine
E-mail: nsc@kipt.kharkov.ua;
[3]V.N. Karazin Kharkiv National University, Kharkov, Ukraine
E-mail: postmaster@univer.kharkov.ua

Irradiation of an industrial aluminum alloy AA1933 with an intense pulsed electron beam with particle energy of 0.35 MeV, a beam current of 2.0 kA, a pulse duration of 5 μs, and a beam diameter of 3 cm results in the formation of a surface layer with a modified structural-phase state. A characteristic feature of the irradiated surface is the presence of cracks and craters on it. This study features the types and morphology of craters on the surface of aluminum alloy AA1933 formed as a result of irradiation by a pulsed electron beam. The study includes figures of a variety of crater types. The distribution of craters according to size and crater density on the irradiated surface was examined. The study also provides for the discussion of the significance of these observations for the sake of a better understanding of the mechanisms of crater formation during irradiation by pulsed electron beams.

PACS: 29.25.Bx, 61.80.Fe, 62.20.−x

INTRODUCTION

Surface modification of materials by concentrated energy flows is successfully used for technological purposes to improve the properties of their surface and near-surface layers [1–12]. Surface treatment of solids by high-current pulsed electron beams (HCPEB) significantly affects their physical and mechanical properties [1–10]. Radiation-induced dynamic thermal fields in the surface layers cause ultrafast heating, melting, and solidification in the process of modifying the surface of materials by pulsed electron beams. In this case, the following processes can occur at the irradiation and high-speed cooling stages: surface layer material melting; heating of material due to heat conductivity; gas-flame cloud formation; formation and propagation of shock waves; redistribution of elements in the recrystallized zone; phase formation under conditions of high-speed crystallization; an increase in the density of dislocations, as well as formation of craters in the surface layers of targets. The combination of these processes determines the state of the surface after pulsed electronic processing and makes it possible to significantly improve the mechanical properties of the material [1–10].

The most characteristic feature of the surface relief of samples treated with a stream of accelerated particles is the presence of defects such as cracks and craters, which can be attributed to the negative consequences of such processing. Craters have been observed by many researchers and are the most common feature on the surface. They are typical of many metal surfaces irradiated by various pulsed energy flows. The formation of craters results in an increase in surface roughness and the formation in the near layer of local regions with highly inhomogeneous stress states [13–15]. It is known that craters are formed as a result of a set of complex physical processes. However, the final answer to the question about the mechanisms and reasons for the formation of craters on the irradiated surface has not yet been found. Further detailed studies of the morphological features of craters, particularly craters resulting from irradiation of various aluminum alloys, are still to be conducted to develop such a mechanism. Such experimental studies are of not only technological but also general scientific interest.

EXPERIMENTAL PROCEDURE

The studied alloy AA1933 has a following chemical composition: Al; 1.6…2.2 wt.% Mg; 0.8…1.2 wt.% Cu; 0.1 wt.% Mn; 0.66…0.15 wt.% Fe; 0.1 wt.% Si; 6.35…7.2 wt.% Zn; 0.03…0.06 wt.% Ti; 0.05 wt.% Cr; 0.10…0.18 wt.% Zr; 0.0001…0.02 wt.% Be [16]. According to the diagram of the Al-Mg-Cu-Zn system state, zinc, magnesium and copper form primary eutectic phases with aluminum and with each other: $MgZn_2$ (η-phase), Al_2CuMg (S-phase), $Mg_3Zn_3Al_2$ (T-phase) [16]. The results of diffraction studies of the underlying microstructure of the AA1933 alloy, performed in [2, 5], made it possible to establish that the underlying microstructure is characterized by the presence of $MgZn_2$ and $Mg_3Zn_3Al_2$ phases, which play a significant role in strengthening the AA1933 alloy in the course of its heat treatment. AA1933 alloy belongs to high-strength alloys. Tensile strength σ_t of AA1933 alloy is 450…520 MPa [16]. The microhardness of the 1933 alloy studied in this work in the initial state is

105*HV*0.50. The microhardness of the irradiated layer of the 1933 alloy, as it was established earlier in [2], is 137*HV*0.50. At elevated temperatures, the alloy shows superplastic behavior [17–21]. At temperature $T = 793$ K and true deformation rate $\dot{\varepsilon} = 1.2 \cdot 10^{-4}$ c^{-1} the elongation of samples of this alloy before destruction is 260% [21].

Plates with a size of 100×100 mm were cut from the sheets of AA1933 alloy with a thickness of 2.5 mm for irradiation. The cladding layer on the plate surface was grinded off, and the plate surface was polished before irradiation. Irradiation of alloy sheets was performed by a HCPEB at the TEMP-A accelerator in the NSC KIPT of the NAS of Ukraine [2, 3, 5]. The energy flux density at the target W is approximately 10^9 W/cm^2 (beam energy E ~ 0.35 MeV, current I ~ 2000 A, pulse duration $\tau_i \sim 5 \cdot 10^{-6}$ s, beam diameter ~ 3 cm). Irradiation was done by the single impulse in a vacuum at $1.3 \cdot 10^{-3}$ Pa. Microstructure studies were performed using a light microscope MIM-6 equipped with digital camera Pro-MicroScan.

RESULTS AND DISCUSSION

When irradiated by HCPEB, the material is rapidly heated to a high temperature. This significantly exceeds the melting point of aluminum alloys [2–7]. Under the action of HCPEB, the heating rate of the alloy is higher in the deep layers. The maximum energy absorption occurs at a depth of approximately 1/3 of the path of electrons in a given substance [13, 14]. This leads to an explosive release of a part of the molten material and subsequent rapid cooling of the alloy by removing heat into the main volume of the target. Understanding the mechanism of crater formation is also essential from the point of view of possible technological applications of release products for surface modification, similar to the process of electric-spark alloying [11, 12]. Cooling is accompanied by crystallization of the molten material and structural-phase transformations. The features of structural-phase changes in the surface layer of industrial aluminum alloy AA1933 of the Al-Mg-Cu-Zn-Zr system irradiated by HCPEB were studied earlier in [2, 5]. In particular, it was established that the formation of a developed relief on the surface of the AA1933 alloy plate and the appearance of microcracks and craters on it accompanies the action of a pulsed electron beam.

Micrographs of typical craters on an irradiated target out of AA1933 alloy are shown in Fig. 1. It should be noted that the craters were distributed fairly evenly over the entire irradiated surface. When craters are isolated and located far enough apart, they tend to take on a regular, round, funnel-shaped shape. Craters are usually multi-ringed. The larger the diameter of the crater, the more multi-ringed it is. Careful visual inspection of the irradiated surface confirms that most of the craters look like those shown in Fig. 1.

The size distribution of craters is an important parameter that can be quantified. Such information, among other things, is of interest when predicting the mechanism of crater formation, which has not yet been fully clarified to date. The diameter of the craters was measured in two mutually perpendicular directions, and the average diameter value was calculated to build such a dependence. The statistical results of the quantitative analysis carried out based on optical micrographs of craters are shown in Fig. 2. The graph shows the size distribution of craters depending on their quantitative fraction. It is evident that the resulting size distribution of craters has an approximately Gaussian form. It is also evident that most of the craters have sizes between 20 and 50 μm. The average diameter of all craters D was determined as 43 μm. Measuring the crater density n and the average crater size D allows determining the ratio of the area occupied by craters on the HCPEB-treated surface S [13]:

$$S = \frac{\pi D^2 n}{4}. \quad (1)$$

This parameter is important for determining the degree of cratering of the HCPEB-modified surface area. Thus, it may be important to determine some properties of surfaces treated this way. The calculated value S for the irradiated surface of the AA1933 alloy is 3.7%. That is, we can say that craters cover an insignificant part of the irradiated surface of the alloy under study.

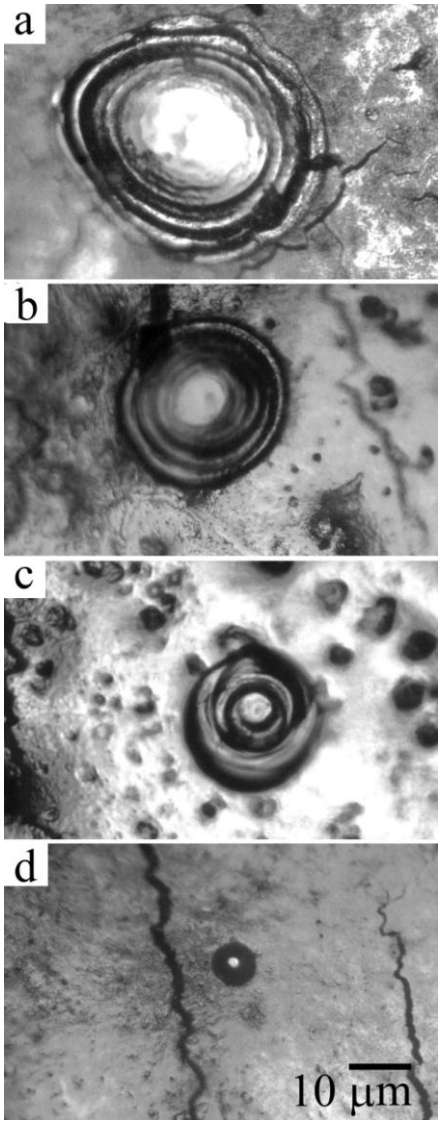

Fig. 1. View of craters on an irradiated target out of AA1933 alloy. The scale is the same for all parts of the figure

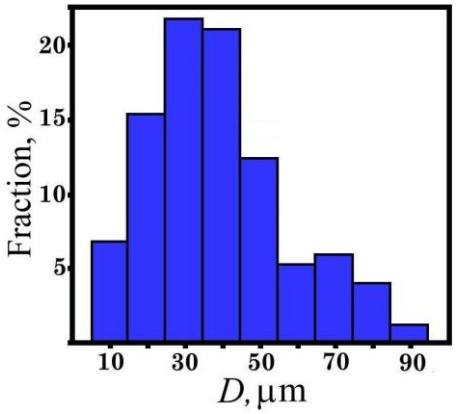

Fig. 2. Size distribution of craters depending on their fraction for an irradiated target out of AA1933 alloy

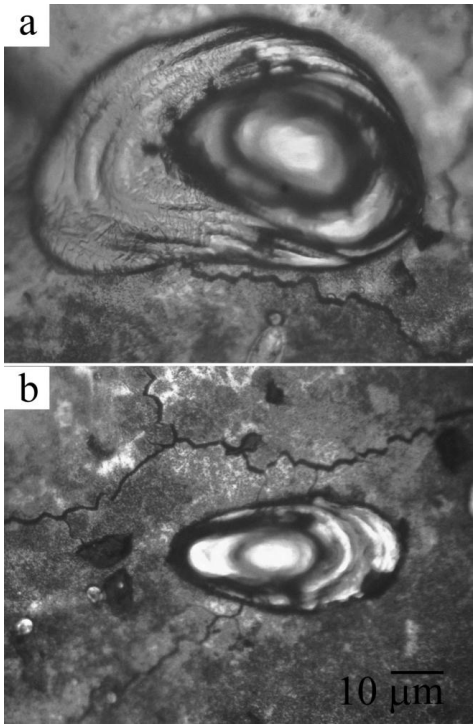

Fig. 3. View of craters on an irradiated target out of AA1933 alloy

However, in addition to the craters described above, there are other craters on the irradiated surface of the AA1933 alloy, the morphology and types of which will be described below. The view of the craters, which, firstly, are not symmetrical, are shown in Fig. 3. Their shape vaguely resembles the form of an ellipse. Secondly, some parts of the molten matter did not pour inside the crater during the crater formation but froze on the surface. The number of such craters is insignificant. Thus, they were not taken into account when building the dependence shown in Fig. 2. However, it cannot be said that these are isolated cases. It is difficult to measure the exact diameter of craters due to their asymmetry. However, it must be noted that there are no craters with small diameters up to 20 μm among such craters.

A more detailed study of the irradiated surface allowed the detection of some other structural features of the craters. A view of the crater, which can be characterized as a three-leaf one, is shown in Fig. 4. The reasons for the formation of such a crater are not yet clear, and craters of this type have not been observed before. Thus, in the future, when predicting the mechanism of crater formation, one should take into account the morphology of the crater shown in Fig. 4,a. Adjacent craters are shown in Fig. 4,b. Each of these craters can no longer be characterized as a crater, but as a throat, out of which liquid poured onto the surface. It should be noted that the craters shown in Fig. 4,b were also extremely rare on the studied surface.

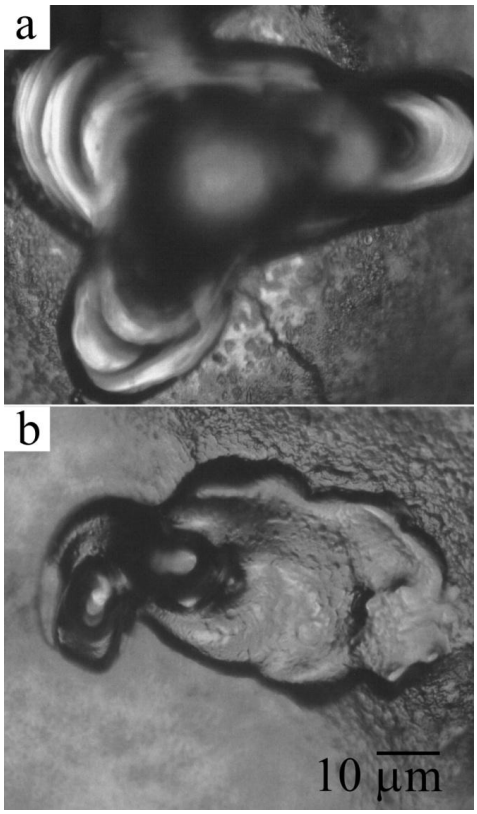

Fig. 4. View of craters on an irradiated target out of AA1933 alloy

Since craters have a significant effect on the surface properties of materials irradiated by pulsed energy flows, clarification of the mechanisms of crater formation is very important for understanding the main processes that occur during HCPEB irradiation and, thus, for predicting possible applications of this technology.

Some remarks can be made regarding the mechanisms of crater formation. The formation of craters on metal surfaces under the influence of pulsed ion beams was mentioned in several studies [1, 22]. In this case, the inhomogeneity of the distribution of ions inside the ion beam leads to the formation of a crater. However, the situation is different in the case of a pulsed electron beam, when the impulse of an individual electron is insignificant, and the beam cross-section is uniform. Based on the numerical simulation of heat flows on aluminum and stainless steel, it was suggested in [13] that the formation of craters during HCPEB irradiation is a consequence of local melting in the layer under the irradiated surface, which causes the subsurface fluid to erupt through the outer surface [22]. It was noted that particles of secondary phases [13] are often centers for the nucleation of local melting and,

thus, centers for crater formation. Indeed, these secondary phase particles usually have a lower thermal conductivity than the matrix, so they melt before the rest of the material. Thus, according to [13], inhomogeneous local melting in the near-surface layer of the target material and subsequent eruption of the molten material through the solid outer surface during processing with a pulsed electron beam is the leading hypothesis for the crater formation. However, in this case, the crater depth shall exceed the thickness of the layer molten by HCPEB, as shown, for example, in [14, 15].

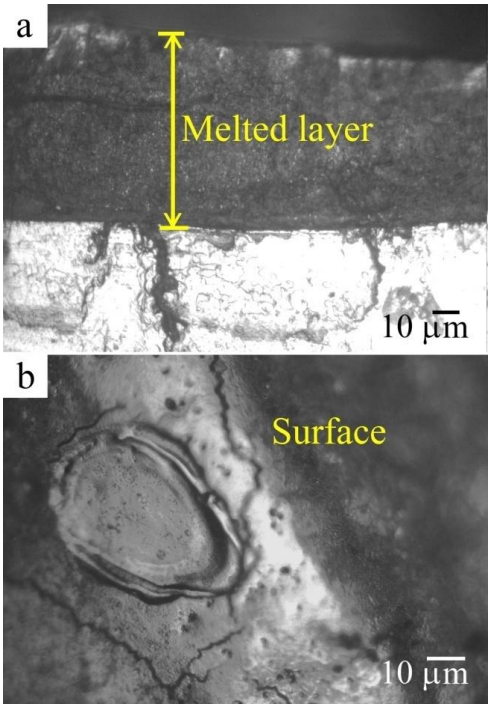

Fig. 5. Cross-sectional view of the 1933 alloy in the electron beam processing zone (a); crater on the irradiated surface of AA1933 alloy (b)

In the case of the AA1933 alloy studied here, the depth of the craters is much less than the thickness of the remelted layer. A cross-sectional view of the AA1933 alloy in the electron beam processing zone is shown in Fig. 5, a. The thickness of the modified layer is about 100 μm on average. The depth of the craters is much less than the thickness of the remelted layer. For example, the depth of the crater on the irradiated surface of the AA1933 alloy, shown in Fig. 5,b, is less than 10 μm. Based on this, it can be assumed that the mechanism of crater formation in this study should be different. At the same time, there may be several other mechanisms for crater formation, considering the presence of craters of various morphologies. At the same time, some of these mechanisms are implemented more intensively, while others are implemented only in some cases. Further research is required to understand the mechanisms of crater formation better.

CONCLUSIONS

1. It was shown that the use of HCPEB results in the formation of craters on the surface of the AA1933 aluminum alloy.

2. Craters are distributed quite evenly over the entire irradiated surface. The size distribution of craters, depending on their quantitative fraction has an approximately Gaussian form.

3. The formation of craters of various morphologies was observed: regular symmetrical rounded funnel-shaped craters, non-symmetrical elliptical craters, and other types of craters.

4. It is essential to take into account the morphology of craters when predicting the mechanism of crater formation. Given the presence of craters of various morphologies, there may be several different mechanisms for crater formation. At the same time, some of these mechanisms are implemented more intensively, while others are implemented only in some cases.

REFERENCES

1. D.I. Proscurovsky, A.D. Pogrebnjak. Modification of metal surface layer properties using pulsed electron beams // *Phys. Stat. Sol. A*. 1994, v. 145, N 1, p. 9-49.

2. V.V. Bryukhovetsky, V.F. Klepikov, V.V. Lytvynenko, D.E. Myla, V.P. Poyda, A.V. Poyda, V.T. Uvarov, Yu.F. Lonin, A.G. Ponomarev. The features of the structural state and phase composition of the surface layer of aluminum alloy Al-Mg-Cu-Zn-Zr irradiated by the high current electron beam // *Nuclear Inst. and Methods in Physics Research B*. 2021, v. 499, p. 25-31.

3. V.V. Bryukhovetsky, V.F. Klepikov, V.V. Lytvynenko, D.E. Myla, Yu.F. Lonin, A.G. Ponomarev. The structural phase state and strength properties of the surface layer of AA6111-T4 aluminum alloy irradiated by the high-current electron beam // *Nuclear Inst. and Methods in Physics Research B*. 2022, v. 519, p. 1-8.

4. Y. Qin, C. Dong, Z. Song, S. Hao, X. Me, J. Li, X. Wang, J. Zou, Th. Grosdidier. Deep Modification of materials by thermal stress wave generated by irradiation of highcurrent pulsed electron beams // *Journal of Vacuum Science and Technology A*. 2009, v. 27, N 3, p. 430-435.

5. D.E. Myla, V.V. Bryukhovetsky, V.V. Lytvynenko, A.V. Poyda, V.F. Klepikov, V.T. Uvarov, Yu.F. Lonin, A.G. Ponomarev. Analysis of changes in the phase and structural state of the surface layer of an aluminum alloy 1933, melted by a pulsed electron beam // *Problems of Atomic Science and Technology*. 2020, N 2(126), p. 33-38.

6. V.V. Bryukhovetsky, A.V. Poyda, V.P. Poyda, D.E. Milaya. Superplastic deformation of the AK4-1 alloy with a surface layer melted by electron pulse beam // *Problems of Atomic Science and Technology*. 2019, N 2(120), p. 67-73.

7. A. Weisenburger, W. An, V. Engelko, A. Heinzel, A. Jianu, F. Lang, G. Mueller, and F. Zimmermann. Intense Pulsed Electron Beams Application of Modified Materials // *Acta Physica Polonica A*. 2009, v. 115, N 6, p. 1053-1055.

8. V.V. Bryukhovetskiy, N.I. Bazaleev, V.F. Klepikov, V.V. Litvinenko, O.E. Bryukhovetskaya, E.M. Prokhorenko, V.T. Uvarov, A.G. Ponomar'ov. Features of gelation of surface of industrial aluminium alloy 6111 in the area of influence of impulsive bunch of electrons in

the mode of pre-melting // *Problems of Atomic Science and Technology*. 2011, N 2(72), p. 28-32.

9. V.V. Bryukhovetsky, V.V. Lytvynenko, D.E. Myla, V.A. Bychko, Yu.F. Lonin, A.G. Ponomarev, V.T. Uvarov. Effect of Structural and Phase Changes under Relativistic Electron Pulsed Beam Irradiation on the Aluminum Alloys Micro-hardness // *Physics and Chemistry of Solid State*. 2021, N 22(4), p. 655-663.

10. D.E. Myla, V.V. Bryukhovetsky, V.V. Lytvynenko, S.I. Petrushenko, O.O. Nevgasimov, Yu.F. Lonin, A.G. Ponomarev, V.T. Uvarov. Microstructure and property modifications in surface layers of a AA6111 aluminum alloy induced by high-current pulsed relativistic electron beam // *Problems of Atomic Science and Technology*. 2022, N 2(138), p. 25-31.

11. V.B. Tarel'nik, V.S. Martsinkovskii, A.N. Zhukov. Increase in the reliability and durability of metal impulse end seals. Part 1 // *Chemical and Petroleum Engineering*. 2017, v. 53, N 1-2, p. 114-120.

12. V. Tarelnyk, V. Martsynkovskyy, O. Gaponova, I. Konoplianchenko, A. Belous, V. Gerasimenko, M. Zakharov. New method for strengthening surfaces of heat treated steel parts // *IOP Conference Series: Materials Science and Engineering*. 2017, v. 233, N 1, art. no. 012048.

13. Y. Qin, Ch. Dong, X. Wang, Sh. Hao, A. Wu, J. Zou, and Y. Liu. Temperature profile and crater formation induced in high-current pulsed electron beam // *Processing Journal of Vacuum Science and Technology A.* 2003, v. 21, N 6, p. 1934-1938.

14. K.M. Zhang, J.X. Zou, T. Grosdidier, C. Dong, Formation and evolution of craters in carbon steels during low-energy high-current pulsed electron-beam treatment // *Journal of Vacuum Science and Technology A.* 2009, v. 27, p. 1217-1226.

15 C. Zhang, J. Cai, P. Lv, Y. Zhang, H. Xia, Q. Guan. Surface microstructure and properties of Cu-C powder metallurgical alloy induced by high-current pulsed electron beam // *J Alloy. Compd*. 2017, v. 697, p. 96-103.

16. I.N. Fridlyander. *Aluminum alloys for aerospace engineering. Today, material knowledge of the 21st century*. Kiev: "Naukova dumka", 1998, 304 p.

17. V.V. Bryukhovetskij. On the origin of high-temperature superplasticity of a coarse-grained avial-type aluminum alloy // *Fizika Metallov i Metallovedenie*. 2001, v. 92, issue 1, p. 107-111 (in Russian).

18. V.V. Bryukhovetsky, R.I. Kuznetsova, N.N. Zhukov, V.P. Poida, V.F. Klepikov. Liquid-phase nucleation and evolution as a cause of superplasticity in alloys of the Al-Ge system *// Phys. Stat. Sol. A.* 2005, v. 202, N 9, p.1740-1750.

19. V.V. Bryukhovetskyy, V.P. Pojda, A.V. Poyda, D.R. Avramets', R.I. Kuznetsova, O.P. Kryshtal', O.L. Samsonnik, K.A. Mahmud. Mechanical properties and structural changes during superplastic deformation of 6111 aluminium alloy // *Metallofiz. Noveishie Tekhnol.* 2009, v. 31, issue 9, p. 1289-1302 (in Russian).

20. A.V. Pojda, V.V. Bryukhovets'ky, D.L. Voronov, R.I. Kuznetsova, V.F. Klepikov. Superplastic behaviour of an AlMg6 alloy at the high homological temperatures // *Metallofiz. Noveishie Tekhnol.* 2005, v. 27, issue 3, p. 317-330 (in Russian).

21. V.P. Poida, D.E. Pedun, V.V. Bryukhovetskii, A.V. Poida, R.V. Sukhov, A.L. Samsonik, V.V. Litvinenko. Structural changes during superplastic deformation of high-strength alloy 1933 of the Al-Mg-Zn-Cu-Zr system // *Phys. Met. Metallogr*. 2013, v. 114, N 9, p. 79-788.

22. V.A. Shulov, N.A. Nochovnaya. Crater formation on the surface of metals and alloys during high power ion beam processing // *Nucl. Instrum. Methods Phys. Res. B, Beam Interact. Mater. Atoms.* 1999, v. 148, p. 154.

Article received 08.12.2022

МОРФОЛОГІЧНІ ОСОБЛИВОСТІ КРАТЕРІВ НА ПОВЕРХНІ АЛЮМІНІЄВОГО СПЛАВУ АА1933, ОПРОМІНЕНОГО ІМПУЛЬСНИМ ПУЧКОМ ЕЛЕКТРОНІВ

В.В. Брюховецький, В.В. Литвиненко, Ю.Ф. Лонін, Д.Є. Мила, А.Г. Пономарьов, В.Т. Уваров

Опромінення промислового алюмінієвого сплаву АА1933 інтенсивним імпульсним електронним пучком з енергією частинок 0,35 МеВ, струмом пучка 2,0 кА, тривалістю імпульсу 5 мкс і діаметром пучка 3 см призводить до формування поверхневого шару з модифікованим структурно-фазовим станом. Характерною особливістю опроміненої поверхні є наявність на ній тріщин та кратерів. У роботі вивчені типи та морфологія кратерів на поверхні алюмінієвого сплаву АА1933, що виникають внаслідок опромінення імпульсним пучком електронів. Показано різноманіття типів кратерів. Досліджено розподіл кратерів за розмірами та щільність кратерів на опроміненій поверхні. Обговорюється значення цих спостережень для більш глибокого розуміння механізмів утворення кратерів у ході опромінення імпульсними пучками електронів.